Influence of soil properties on amplification of saturated inhomogeneous poroviscoelastic soil profile

Authors:

Toufiq Ouzandja, PhD. CE
University A. Mira Bejaia
Faculty of Technology
Laboratory of Construction Engineering and Architecture (LGCA), Algeria
National Earthquake Engineering Research Centre (CGS), Seismic Hazard Division, Algeria
ouzandja.toufiq@yahoo.fr
Corresponding author

Prof. **Mohamed Hadid**, PhD. CE
Ecole Nationale Supérieure des travaux Publics
Laboratoire des Travaux Publics Ingénierie de Transport et Environnement (TPiTE), Algeria
hadid_mohamed2003@yahoo.fr

Research paper

Toufiq Ouzandja, Mohamed Hadid

Influence of soil properties on amplification of saturated inhomogeneous poroviscoelastic soil profile

The influence of local geotechnical site conditions on the soil profile amplification is analysed in this paper by assuming that the incoming seismic waves consist of inclined P-SV waves. The inhomogeneous soil profile is idealized as a multi-layered saturated poroviscoelastic medium and characterized by the Biot's theory with a shear modulus varying continuously in depth according to the Wichtmann's model. The results are presented in terms of horizontal and vertical soil profile amplification with linear and nonlinear soil behaviour, for different values of incidence angle, pore-water saturation, porosity, permeability, coefficient of uniformity, and non-cohesive fines content.

Key words:
Biot's theory, amplification function, nonlinear soil behaviour, inhomogeneous soil profile

Prethodno priopćenje

Toufiq Ouzandja, Mohamed Hadid

Utjecaj svojstava tla na amplifikaciju zasićenog nehomogenog porovisko-elastičnog profila tla

U radu se analizira utjecaj lokalnih geotehničkih uvjeta tla na amplifikaciju profila tla uz pretpostavku da se dolazni seizmički valovi sastoje od kosih P-SV valova. Nehomogeni profil tla idealizira se kao višeslojni zasićeni poroviskoelastični medij karakteriziran Biotovom teorijom, pri čemu modul posmika kontinuirano varira po dubini u skladu s Wichtmannovim modelom. Rezultati su iskazani u vidu horizontalne i vertikalne amplifikacije profila tla pri linearnom i nelinearnom ponašanju tla, za razne vrijednosti upadnog kuta, stupnja zasićenosti, poroznosti, propusnosti, koeficijenta jednolikosti i udjela sitnih nekoherentnih čestica.

Ključne riječi:
Biotova teorija, funkcija amplifikacije, nelinearno ponašanje tla, nehomogeni profil tla

Vorherige Mitteilung

Toufiq Ouzandja, Mohamed Hadid

Einfluss der Bodeneigenschaften auf die Verstärkung des gesättigten inhomogenen porös-elastischen Bodenprofils

Die Abhandlung analysiert den Einfluss lokaler geotechnischer Bedingungen auf die Verstärkung des Bodenprofils, unter der Voraussetzung, dass die ankommenden seismischen Wellen aus schrägen P-SV-Wellen bestehen. Das inhomogene Bodenprofil wird als mehrschichtiges gesättigtes porös-elastisches Medium idealisiert, das durch die Biot-Theorie charakterisiert ist, wobei das Schermodul gemäß dem Wichtmann-Modell kontinuierlich in der Tiefe variiert. Die Ergebnisse werden in Form einer horizontalen und vertikalen Verstärkung des Bodenprofils bei linearem und nicht linearem Bodenverhalten für verschiedene Werte des Einfallswinkels, Sättigungsgrads, Porosität, Durchlässigkeit, des Gleichmäßigkeitskoeffizienten und Anteile kleiner inkohärenter Partikel dargestellt.

Schlüsselwörter:
Biot-Theorie, Verstärkungsfunktion, nicht lineares Bodenverhalten, inhomogenes Bodenprofil

1. Introduction

Local site conditions play a significant role in the earthquake response of structures supported by soft soil [1]. Therefore, a rigorous earthquake resistant design of structures should take into account structural complexity of underground soil (stratification, porosity, inhomogeneity of shear modulus, saturation degree, permeability...), which is responsible for multiple alterations that affect seismic waves during their propagation from the source to the top surface.

In most natural soil deposits, mechanical properties and stiffness increase with their distance from the surface [2-8]. The experience has shown that in such soil the shear modulus values vary exponentially with depth due to the confining effect of overburden. Several researchers have evaluated the seismic response of soil deposits to incident plane waves, with the focus on continuous variation of mechanical properties of soil. The soil profile is called an inhomogeneous soil profile and it is assumed that its shear modulus increases with some power exponent of depth [9-19]. However, all these studies are applicable to the one phase solid media only, and cannot be applied for more realistic soils which are often present in the form of fluid-saturated poroviscoelastic media in nature. Due to substantial computational effort required to obtain the response of an inhomogeneous saturated poroviscoelastic soil profile, very few studies applying the Biot's theory have so far been written [20-22]. Based on this theory, the complex dispersion equation for Love waves is derived for transversely isotropic fluid-saturated porous media with exponential and linear variation of shear modulus [23-24]. The dispersion behaviour of plane wave [25], Rayleigh wave [26] and transient response of viscoelastic porous medium [27], are analysed in the inhomogeneous saturated soil with gradient variation of mechanical properties along the depth. However, it should be noted that none of these studies examine the problem of amplification of the porous soil response. In addition, the formulas proposed in these studies for describing the inhomogeneous shear modulus of the saturated porous soil profile are not realistic, and they do not take into account geotechnical site conditions, such as soil classification (sand, clay ...), degree of saturation, grain size distribution, fines contents, etc., which can play a significant role in the soil profile amplification.

The effect of grain size distribution in terms of coefficient of uniformity, degree of saturation, porosity, permeability, and fines content, on both horizontal and vertical soil amplification with linear and nonlinear soil behaviour, is presented in this paper. The soil profile is idealized as a multi-layered saturated poroviscoelastic medium and characterized by Biot's theory in conjunction with the Witchman model [6-8] which consider the shear modulus varying continuously with depth and take into consideration the effect of the grain size distribution, porosity and fines content on dynamic properties of sandy soil.

The analysis of seismic response is carried out via the exact stiffness matrix method in frequency domain [28], assuming that the incoming seismic waves consist of inclined *P-SV* waves. The stiffness matrix method used in this paper appears to be well suited for treating poroviscoelastic soil amplification problems. The method is highly beneficial as it provides a significant benefit in reducing the number of calculations operations compared to the numerical methods, while automatically accounting for the radiation condition.

2. Soil model description

The motion in soil is assumed to be governed by the Biot's two-phase theory of wave propagation in a saturated poroelastic homogeneous material, which is based on the assumption that the motion of the solid matrix is a wave motion, whereas, that of the fluid relative to the solid is a diffusion process described by Darcy's law. According to Biot's theory, the constitutive relations of a homogeneous poroelastic medium in a Cartesian coordinate system can be expressed as:

$$\sigma_{ij} = \lambda e \delta_{ij} + 2G\varepsilon_{ij} - \alpha p \delta_{ij} \quad i, j = x, z \tag{1}$$

$$p = -\alpha M e + M\zeta \tag{2}$$

In the above equations, σ_{ij} is the total stress tensor of solid skeleton and ε_{ij} is the strain tensor; $e = div\ u$ and $\zeta = -div\ w$ denote, respectively, the dilatation components of the solid frame and the increment of fluid content; p is the pore fluid pressure, λ and G are Lame constants of the bulk material, δ_{ij} is the Kronecker delta, α and M are the Biot's parameters accounting for the compressibility of grains and fluid (0 ≤ α ≤ 1 and 0 ≤ M ≤ ∞), and can be given as:

$$K_b = \lambda + \frac{2}{3}G \tag{3}$$

$$\alpha = 1 - \frac{K_b}{K_s} \tag{4}$$

$$\frac{1}{M} = \frac{\alpha - n}{K_s} + \frac{n}{K_f} \tag{5}$$

$$\frac{1}{K_f} = \frac{1}{K_w} + \frac{1 - S_r}{P_a} \tag{6}$$

K_s, K_b, K_w and K_f are the bulk modulus of solid grains, skeleton, pore water and pore fluid, respectively. P_a is the absolute fluid pressure, n is the porosity, and S_r is the degree of saturation (0.95 ≤ S_r ≤ 1).

Therefore, in terms of the displacement of the solid frame, u, and the fluid relative to the solid frame, w, the wave motion equations can be written in the following form [29]:

For the solid skeleton:

$$G\nabla^2 u + \left(\lambda + \alpha^2 M + G\right)\nabla e - \alpha M \nabla \zeta = \rho \ddot{u} + \rho_f \ddot{w} \tag{7}$$

For the pore fluid:

$$\alpha M \nabla e - M \nabla \zeta = \rho_f \ddot{u} + m \ddot{w} + b \dot{w} \tag{8}$$

ρ is the density of the porous matrix and is expressed by $\rho = (1-n) \rho_s + n\rho_f$, where ρ_s and ρ_f are the densities of the solid phase and liquid phase, respectively. $b = \eta/k$ is the parameter accounting for the internal friction due to relative motion between the solid and the pore fluid ($b = 0$, the flow damping is neglected) where η is the fluid viscosity and k is the permeability (m^2). $m = \tau\rho_f/n$ is a parameter related to the mass density of the pore fluid and the pore geometrical features, and τ is the static tortuosity coefficient (geometrical sinuosity of porous medium) for the inertia induced by solid-fluid interaction, depending on the shape of solid grain particles [30, 31].

$$\tau = 1 + r\left(\frac{1}{n}-1\right) \quad \text{in the case of spherical solid grains, r = 0,5} \quad (9)$$

Moreover, the velocities of the three types of waves existing in a saturated porous medium (V_{sv}, V_{p1} and V_{p2}) can be computed using the following expressions [28]:

$$V_{sv} = \sqrt{\frac{G(ib-\omega m)}{\omega\left(\rho_f^2 - \rho m\right) + i\rho b}} \quad (10)$$

$$V_{p_{1,2}} = \frac{\omega}{k_{p_{1,2}}} \quad (11)$$

$$k_{p_1}^2 = \frac{-\varpi_1 + \sqrt{\varpi_1^2 - 4\varpi_2}}{2}, \quad k_{p_2}^2 = \frac{-\varpi_1 - \sqrt{\varpi_1^2 - 4\varpi_2}}{2} \quad (12)$$

where

$$\varpi_1 = \frac{\left(\lambda + 2G + \alpha^2 M\right)\left(ib\omega - m\omega^2\right) + \left(2\rho_f\alpha - \rho\right)\omega^2 M}{\left(\lambda + 2G\right)M} \quad (13)$$

$$\varpi_2 = \frac{\omega^4\left(\rho m - \rho_f^2\right) - ib\rho\omega^3}{\left(\lambda + 2G\right)M} \quad (14)$$

with an angular frequency expressed as ω.

On the other hand, taking into account the inhomogeneity of mechanical properties of soil profile considered in this study, the site is considered as an inhomogeneous sandy soil profile. The shear modulus increases in the depth according to the Witchman's model, in which the Hardin's equations [2] are extended to include the influence of the grain size distribution [6] in terms of the coefficient of uniformity C_u, as well as the non-cohesive fines content effect FC, [8]. Then, the small strain shear modulus is estimated from the following simple equation:

$$G_{max} = A\frac{(a-e_1)^2}{1+e_1}\left(\frac{\sigma_0'}{P_{atm}}\right)^{n'} P_{atm} \quad (15)$$

where

$$a = 1.94\exp(-0.066\,C_u)\exp(0.065\,FC) \quad (16)$$

$$n' = 0.40\,C_u^{0.18}\left[1+0.116\,\ln(1+FC)\right] \quad (17)$$

$$A = (1563+3.13\,C_u^{2.98})$$
$$\frac{1}{2}\left[\exp(-0.3\,FC^{1.1})+\exp(-0.28\,FC^{0.85})\right] \quad (18)$$

$$\sigma_0' = \frac{\sigma_v'}{3}(3-2\sin\phi') \quad (19)$$

and where the following symbols are used: void ratio e_1 ($e_1 = n/(1-n)$), friction angle ϕ', vertical stress σ_v', mean pressure σ_0' and atmospheric pressure $P_{atm} = 100$ kPa.

It is assumed in this study that the soil profile has mechanical properties (stiffness, shear modulus,) that increase with some power exponent of depth (z), according to the increase of confining effect of overburden, which is presented by the vertical stress σ_v' ($\sigma_v' = \gamma'z$), (γ': specific weight). Moreover, to additionally explain the shear modulus-dependent depth, the equation (15) of G_{max} has been rewritten in the form dependant on depth (z):

$$G_{max}(z) = G_0\left(\frac{z}{H}\right)^{n'} \quad (20)$$

where

$$G_0 = A\frac{(a-e_1)^2}{1+e_1}\left(\frac{\frac{\gamma'H}{3}(3-2\sin\phi')}{P_{atm}}\right)^{n'} P_{atm} \quad (21)$$

Here H is the soil profile thickness and G_0 is the shear modulus at the bottom (Figure 1).
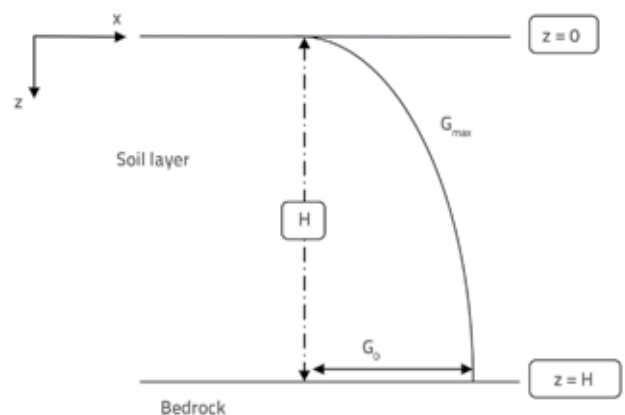

Figure 1. Variation of shear modulus G_{max} with the depth

In addition, the Poisson ratio can be expressed as follows [7, 8, 32]:

$$v = \frac{\alpha'}{4(1-\alpha')} + \sqrt{\left(\frac{\alpha'}{4(1-\alpha')}\right)^2 - \frac{\alpha'-2}{2(1-\alpha')}}, \quad \alpha' = \frac{M_{max}}{G_{max}} \quad (22)$$

with the constrained elastic modulus M_{max} expressed for sands by the following equation (23):

$$M_{max} = A_1 \frac{(a_1 - e_1)^2}{1 + e_1} \left(\frac{\sigma'_0}{P_{atm}} \right)^{n'_1} P_{atm} \qquad (23)$$

where

$$a_1 = 2.16 \exp(-0.055 \ C_u)(1 + 0.116 \ FC) \qquad (24)$$

$$n'_1 = 0.344 \ C_u^{0.126}(1 + 0.125 \ \ln(1 + FC)) \qquad (25)$$

$$A_1 = (3655 + 26.7 \ C_u^{2.42})$$
$$\frac{1}{2} \Big[\exp(-0.42 \ FC^{1.10}) + \exp(-0.52 \ FC^{0.6}) \Big] \qquad (26)$$

Furthermore, it should be noted that the damping effects considered in the above constitutive equations are caused only by the interaction of the viscous fluid and the elastic solid, but the material damping due to the friction between solid grains always exists. The poroviscoelastic and relaxation properties are assumed by replacing the elastic coefficients λ, G and M by complex moduli λ^*, G^*, and M^* [33].

$$G^* = G(1 + 2i\xi_\mu) \qquad (27)$$

$$\lambda^* = \lambda(1 + 2i\xi_\mu) \qquad (28)$$

$$M^* = M(1 + 2i\xi_M) \qquad (29)$$

ξ_μ is the hysteretic damping ratio and

$$\xi_M = \xi_\mu \frac{(\alpha - n)}{(\alpha - n) + n\dfrac{K_s}{K_f}},$$ which can be derived from equation (5).

3. Validation and reliability of the method used

It is already known that the vertical propagation of SV wave exhibits an identical behaviour to that of SH vertical propagation case. We can therefore make comparisons with the corresponding results of the common 1-D upwards shear waves method. For this purpose, we consider a poroviscoelastic saturated single layer soil profile overlying a half space and subjected to the vertical SV wave propagation. The soil profile properties are summarized in Table 1. The results of the proposed method (stiffness matrix method) in terms of horizontal amplification at the surface are compared with those evaluated by the DEEPSOIL software, which assumes a vertical propagation of SH wave.

Horizontal amplification curves given in Figure 2 show that the results obtained by means of the proposed method (vertical SV wave propagation) are in perfect agreement with those obtained by DEEPSOIL.

Table 1. Soil properties of fluid-saturated porous soil profile-bedrock system

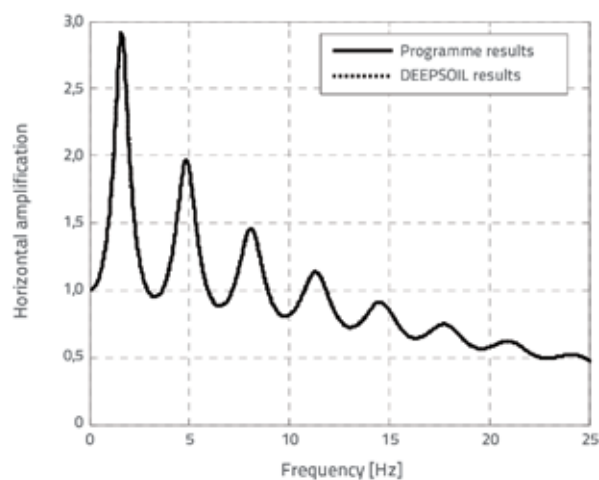| Properties	Sand	Half space
Thickness H [m]	30	/
Shear modulus G [MPa]	80	1000
Permeability k [m²]	10^{-10}	10^{-13}
Porosity n	0.3	0.1
Solid grains density ρ_s [kg/m³]	2600	2600
Bulk modulus of solid grains K_s [GPa]	36	36
Bulk modulus of pore water K_w [GPa]	2.2	2.2
Fluid viscosity η (Ns/m²)	10^{-3}	10^{-3}
Pore-water saturation [%]	100	100
Damping ξ_μ [%]	5	1
Poisson's ratio	0.3	0.3

Figure 2. Comparison of horizontal amplification at the surface between the proposed method and DEEPSOIL results

To verify the benefits of the proposed method, the vertical response of Kobe's Port Island in the 1995 Kobe earthquake was also simulated, using the soil properties and wave velocities for different layers given in table 2 [34, 35], and assuming a vertical incident of plane P wave. Moreover, the up–down component seismic accelerograms recorded at the port island site at a depth of 83 m were selected as input motions (Figure 3). The results obtained by the stiffness matrix method were also compared with the results recorded in situ.

It can be observed that variation in the shear wave velocities profile (V_s) is not significant, which implies that the soil stiffness gradually decreases from the base to the surface. However, a significant decrease of P wave velocities (from 1480 m/s to 780 m/s) appears approximately at a depth 12.6 m. This decrease can be explained by the effect of pore water saturation on the P wave velocity (section 4.1.2). For this purpose, the soil is assumed in this simulation to be fully saturated below the depth of 12.6 m and partly saturated above that level.

Table 2. Soil properties and wave velocities (Kobe's Port island site)

Depth [m]	Thickness [m]	Density [kN/m³]	V_P [m/s]	Damping factor [%]	V_S [m/s]
0-2	2	1.8	260	17	170
2-5	3	1.8	330	17	170
5-12.6	7.6	1.8	780	17	210
12.6-19	6.4	1.8	1480	10	210
19-27	8	1.5	1180	10	180
27-23	6	1.85	1330	10	245
33-50	17	1.85	1530	10	305
50-61	11	1.85	1610	10	350
61-79	18	1.8	1610	10	303
79-83	4	1.9	2000	10	320

The comparison between the evaluated response and the recorded one is presented in terms of spectral ratios of accelerations at the surface and at a depth of 83 m (Figure 4). The comparison between vertical acceleration at ground surface and vertical peak ground acceleration profile is presented in Figure 5. It can be seen that the results obtained by vertical response analysis are in good agreement with those recorded at Port Island, Kobe.

Figure 4. Comparison of spectral ratios of vertical accelerations at the surface and at a depth of 83 m

4. Parametric study

4.1. Linear analysis

A parametric study is presented in this section in order to analyse the effect of variation in incidence angle, pore-water saturation, coefficient of uniformity, fines content, porosity, and permeability on the bi-directional
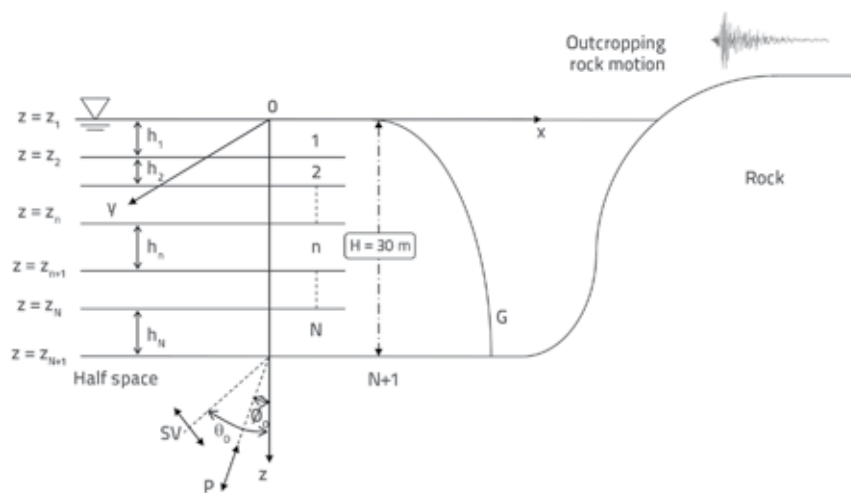

Figure 3. Vertical component of acceleration recorded at a depth of 83 m (port island site)
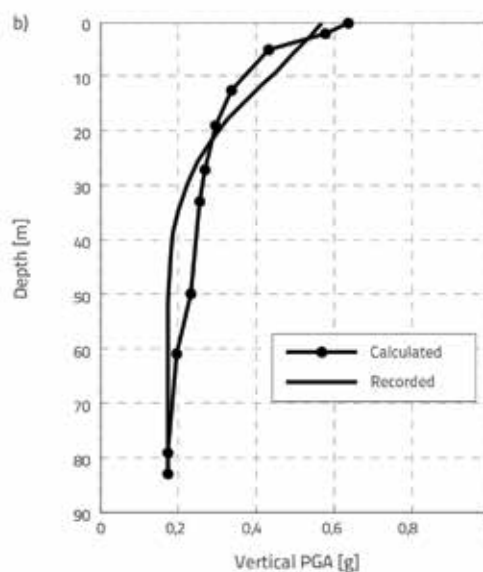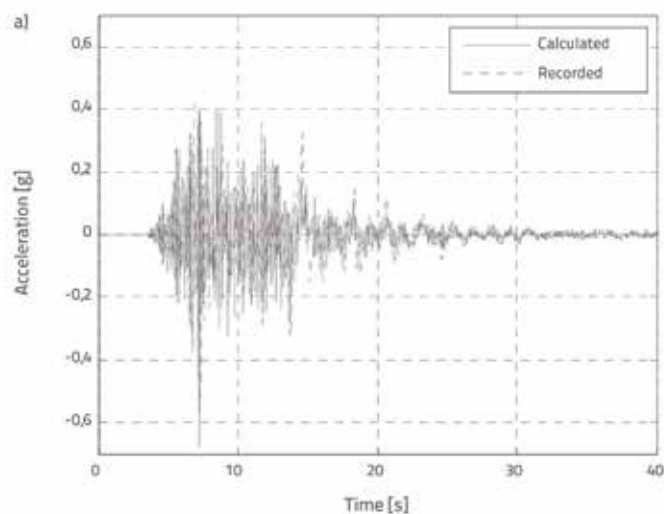
Figure 5. Comparison of: a) vertical acceleration at ground surface; b) vertical peak ground acceleration profile

Figure 6. Geometry of soil profile

amplification response of poroviscoelastic soil profile, whereas, this amplification is given by the ratio of motion at the ground surface and at an outcropping half space. For this propose, It is assumed that the soil profile is an inhomogeneous single 30m sandy soil layer overlying a rock formation, and it is discretized into multiple layers that exhibit constant properties within each sub-layer (Figure 6). The excitation consists of incident plane P and SV waves having different incidence angles and coming from a half space ($Ø_0$ and θ_0 are the incidence angles of plane P and SV waves, respectively). It is also assumed that the horizontal and vertical responses are due only to the propagation of SV and the P waves, respectively. In this paper, both soil profile and half space are considered as a poroviscoelastic material and are characterized by its degree of saturation S_r, porosity n, permeability k, damping ξ_M and ξ_μ (ξ_μ is the hysteretic damping ratio, assumed to be the same for both SV and P waves), the compressibility of solid and fluid constituents. The properties of the sand and rock used in this computation are summarized in Table 3.

Table 3. Soil properties of fluid-saturated porous soil-bedrock system

Properties	Sand	Half space
Thickness H [m]	30	/
Shear modulus G [GPa]	/	1.5
Permeability k [m²]	10^{-10}–10^{-13}	10^{-13}
Porosity n	0.2–0.4	0.05
Solid grains density ρ_s [kg/m³]	2600	2600
Bulk modulus of solid grains K_s [GPa]	36	36
Bulk modulus of pore water K_w [GPa]	2.2	2.2
Fluid viscosity η [Ns/m²]	10^{-3}	10^{-3}
Damping ξ_μ [%]	5	1
Friction angle ϕ'	35°	/

4.1.1. Effect of incidence angle

The effect of incidence angles ($Ø_0$ and θ_0) on both horizontal and vertical soil amplification of a poroviscoelastic soil profile is first considered (Figure 6). It is assumed that the incident waves impinge the soil profile-half space interface at 0°, 10° and 20° with respect to the vertical axis z.

The analysis of amplification functions shown in Figure 7 indicates that the effect of variation in incident angle $Ø_0$ on the vertical amplification for a plane P-wave incoming in fully saturated porous medium is negligible. In the same media, for a plane SV-wave incident, the horizontal amplification is influenced by incidence angle θ_0 (Figure 8.a). This influence is more pronounced in the case of the porous medium than in the solid medium (Figure 8b). It was also observed that the two horizontal soil amplifications in porous and solid media are identical for vertical SV-wave propagation (Figures 8.a and 8.b).

Moreover, the increase of the SV-wave incidence angle θ_0, has reduced the amplification. Thus, the amplification peak is equal to 3.71 with a fundamental frequency equal to 1.8 Hz when $\theta_0 = 0°$. Then it drops to 3.6 and 3.23 in the single-phase medium, and also to 3.52 and 2.7 in the fluid-saturated porous medium, when θ_0 becomes 10° and 20° respectively. This difference could be explained by the fact that the P-SV conversion is not the same for the solid and saturated porous media (Figure 9). When the SV wave presents an angle of incidence different from zero in the saturated porous media, it generates the fast compressional wave (P_1 wave) and the shear wave (SV wave), similar to the corresponding ones in the single-phase medium, and also the slow compressional wave (P_2 wave) associated with the out-of-phase movement between pore fluid and solid phase [36].

In the following parametric study, it is assumed that the incidence angles ($Ø_0$ and θ_0) are equal to 10° with respect to the vertical axis for both P and SV waves.

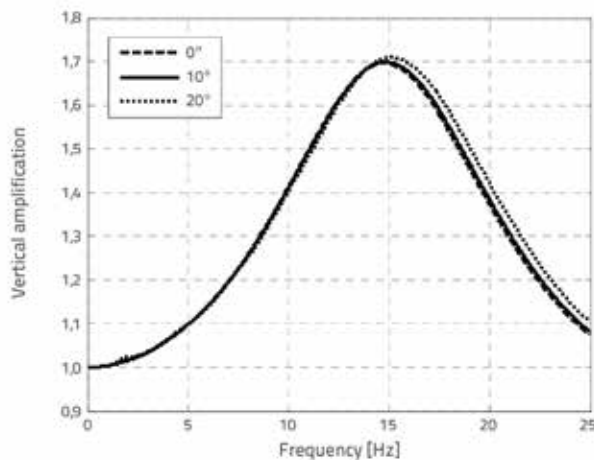**Figure 7. Effect of incidence angle on vertical amplification in fully saturated porous medium (**$n = 0,3$, $C_u = 5$, $FC = 5$ %, $S_r = 100$ %**)**
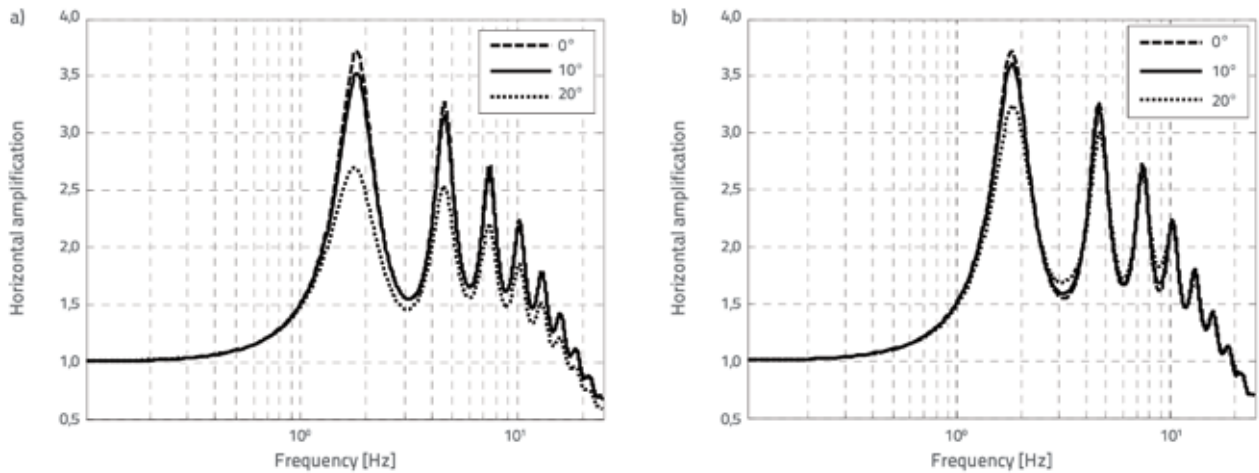
Figure 8. Effect of incidence angle on horizontal amplification: a) fully saturated porous soil (n = 0.3, C_u = 5, FC = 5 %, S_r = 100 %); b) solid medium
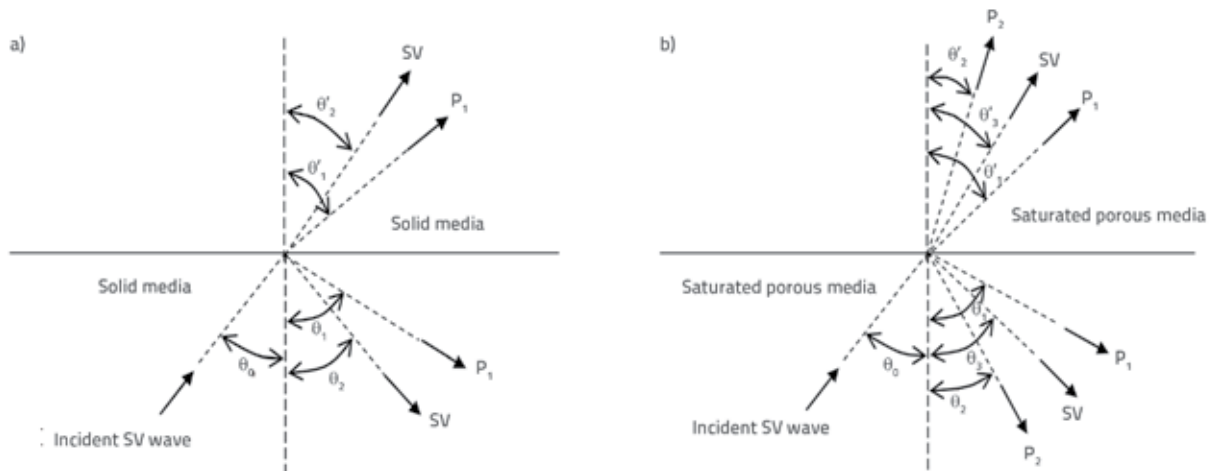

Figure 9. Reflection and transmission of SV waves: a) in solid; b) fluid saturated porous medium

4.1.2. Effect of pore-water saturation

In geotechnical analyses, most studies assume that the soil below the groundwater table is fully saturated. however, under some conditions affecting the location of water table, the subsoil becomes incompletely saturated. This difference is due to the existence of air embedded in pore fluid for a partly saturated case. This air proportion influences largely the bulk modulus of the pore fluid (Equation 6).

As shown in Figure 10, the pore fluid modulus K_f is equal to the pore water modulus (2200 Mpa) for S_r = 100 %, but it is decreases by 99.9 % when S_r becomes 95 %. As the partial saturation reduces the bulk modulus of the pore fluid significantly, the assumption of the incompressibility of the fluid, generally adopted in soil mechanics, is quite inappropriate in this case.

In order to account for the effect of saturation on the site response, both seismic wave's velocities and site amplification are analysed. It should be noted that only the velocity of P waves (V_{P1} and V_{P2}) is affected by the degree of saturation.
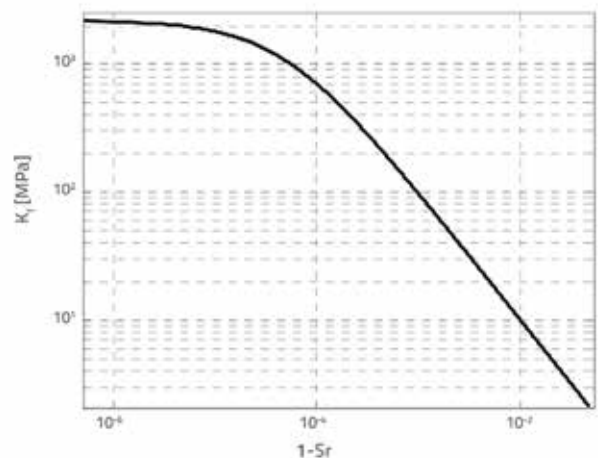
Figure 10. Fluid modulus variation with saturation S_r

Figure 11a shows that V_{p1} is maximal (V_{p1} = 1756 m/s) for the case of full saturation, but it is strongly reduced when S_r becomes 95 % (V_{p1} = 365 m/s), which is in accordance
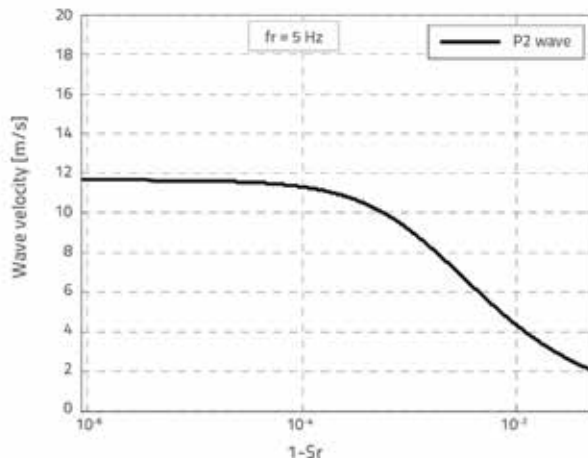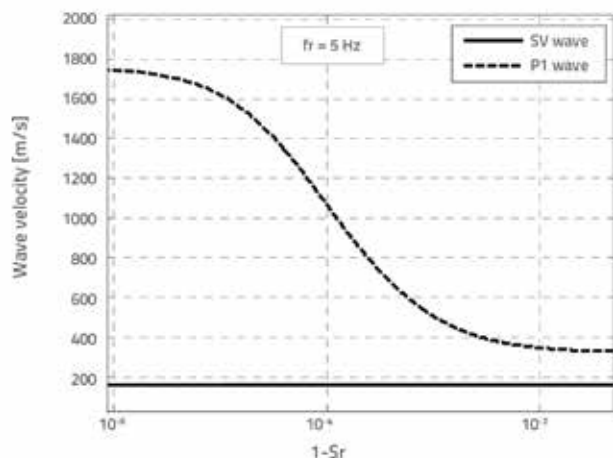
Figure 11. Effect of saturation (σ'_0 = 100 *kPa*, C_u = 5, *FC* = 5 %) on wave velocity: a) wave SV and P1; b) P2 wave

with the saturation-dependent pores fluid modulus. The P_2 wave is highly dispersive and tends to attenuate at low frequencies (Figure 11b). Furthermore, the *SV* wave velocity is not influenced by the degree of saturation (Figure 11a).

On the other hand, the results for horizontal and vertical amplification in these four cases of saturation indicate that the influence of water saturation on the horizontal amplification is negligible (Figure 12). This is completely logical since only the compressional waves propagate in the interstitial fluid, but its effect is very notable on the vertical amplification (Figure 13). For a weak decrease below complete saturation (99.9 %), the vertical amplification increases strongly from 1.7 to 3, with a significant shifting of the frequency of the first peak to the low- frequencies from 14.84 Hz to 4.66 Hz.
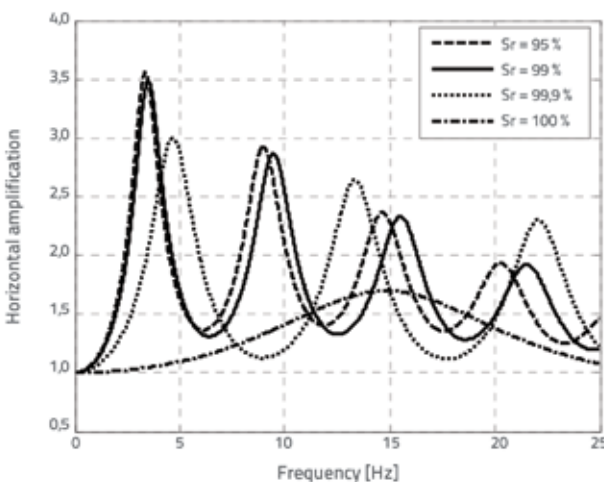
Figure 13. Effect of saturation on vertical amplification (*n* = 0.3, C_u = 5, *FC* = 5 %)

4.1.3. Effect of grain size distribution

In terms of the coefficient of uniformity, the grain size distribution plays a key role in soil mechanics and geotechnical engineering. It constitutes an important factor for evaluating the shear modulus of soil. For small C_u-values, the soil is considered to be poorly graded or uniformly graded, as the size of the soil particles are nearly identical. However, with an increase in C_u – values, the shear modulus decreases and the soil become well graded.

On the other hand, the amplification functions are presented for different C_u-values, C_u = 2, 5 and 8; it has been shown that, as the coefficient of uniformity C_u increases, the amplitude of peaks increases with a shift to low frequencies for horizontal amplification, and also for the vertical one in the case of a partly saturated soil profile (Figure 14). Yet, the vertical component of amplification is not affected in a fully saturated case (Figure 15).
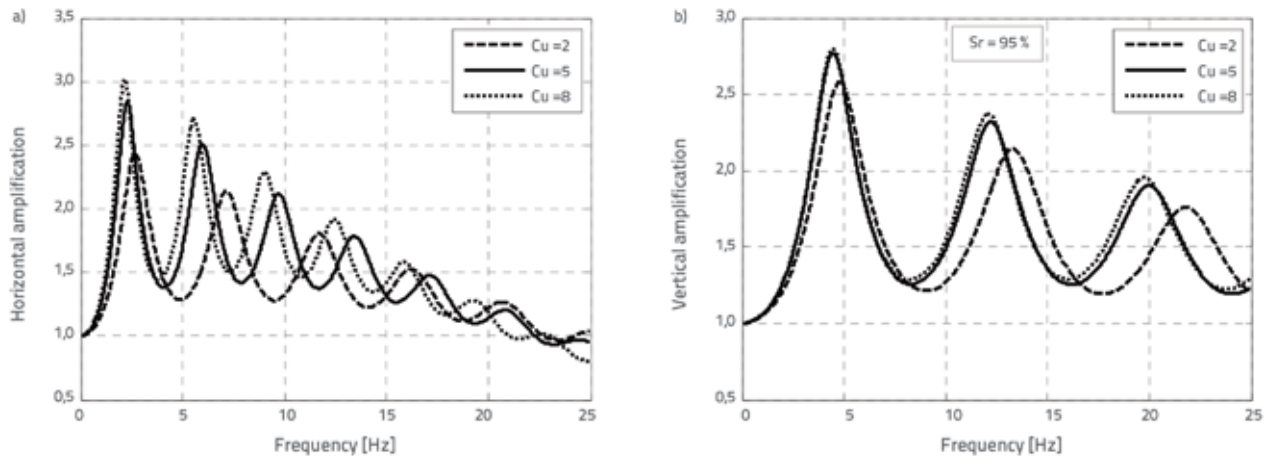

Figure 12. Effect of saturation on horizontal amplification (*n* = 0.3, C_u = 5, *FC* = 5 %)

Figure 14. Effect of C_u-values on: a) the horizontal; b) vertical amplification (S_r = 95 %, FC = 0 %, n = 0.3)
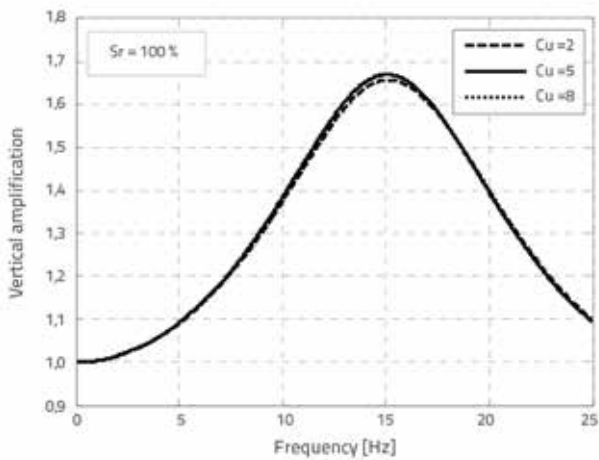

Figure 15. Effect of C_u on the vertical amplification (FC = 0 %, n = 0.3, S_r = 100 %)

To further investigate this effect, seismic wave velocities are illustrated as a function of C_u-values. It can be noticed that when C_u increases from 2 to 8, P_1 wave velocity is reduced by 8.5 % and

less than 1 % for partly and fully saturated medium, respectively (Figure 16), which may explain the small C_u-effect on the vertical amplification when S_r = 100 %. However, the SV wave velocity also reduces in the same manner in partly and fully saturated cases (Figure 17).
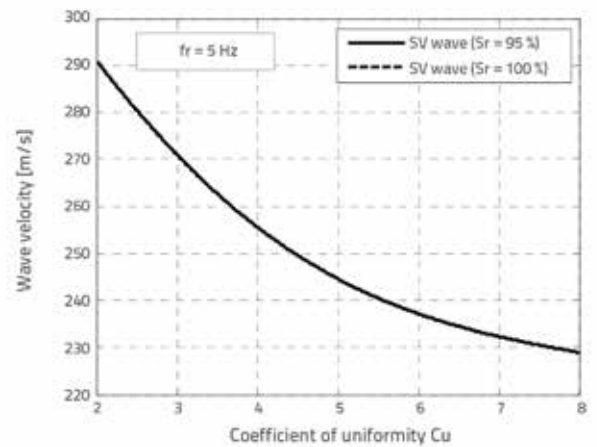
Figure 17. Effect of C_u-values on SV wave velocity (σ'_0 = 100 kPa, FC = 0 %, n = 0.3)
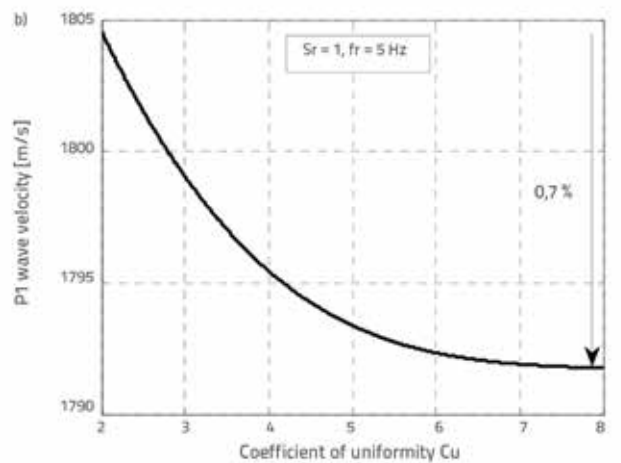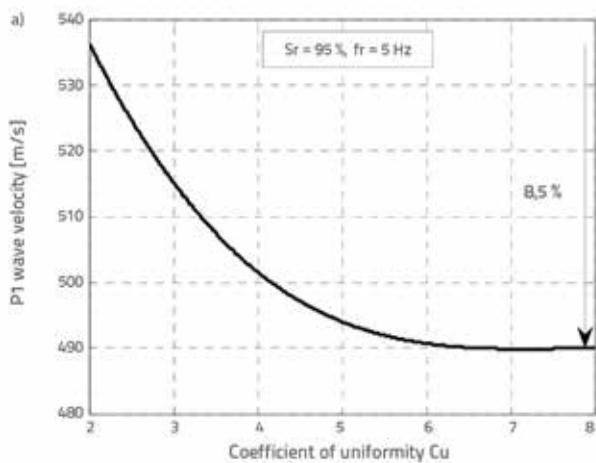

Figure 16. Effect of C_u-values on P_1 wave velocity in: a) partly; b) fully saturated porous soil (σ'_0 = 100 kPa, FC = 0 %, n = 0.3)
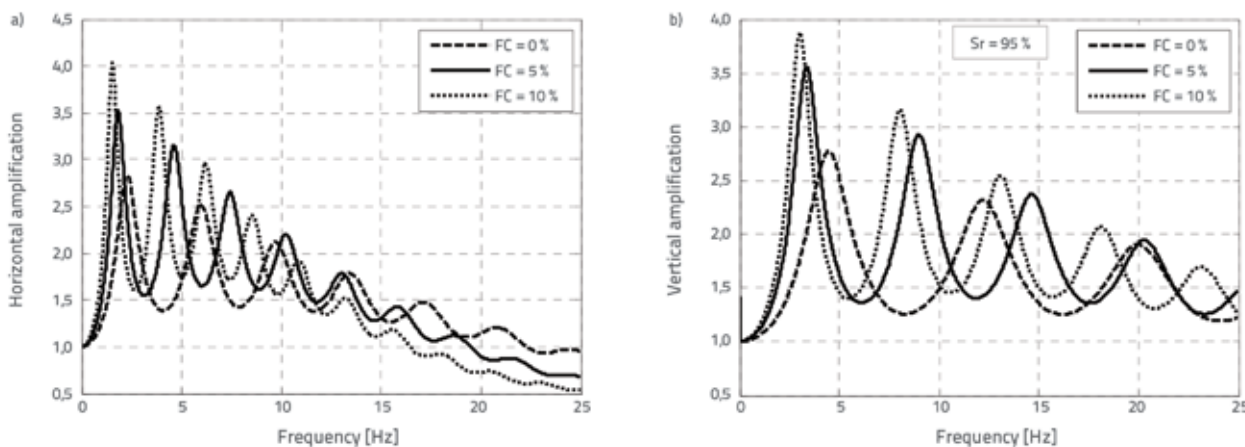
Figure 18. Effect of FC-values on: a) the horizontal; b) vertical amplification (S_r = 95 %, C_u = 5, n = 0.3)

4.1.4. Effect of non-cohesive fines content

Several investigations on the presence of plastic or non-plastic fine content in the sandy soil are focused on the soil liquefaction resistance [37, 38] and often neglect the impact of this fine content on the amplification of soil response. For this purpose, it is assumed in this study, that the shear modulus depends of the non-cohesive fines content according to the Wichtmann's model [8].

Both horizontal and vertical amplification with S_r = 95 % exhibit variations similar to those obtained in C_u-analysis, in which the increase of FC-values induces an increase of amplification peaks with a shift to low frequencies (Figure 18). However, the vertical amplification in the completely saturated soil is slightly influenced by the fines content values (Figure 19).
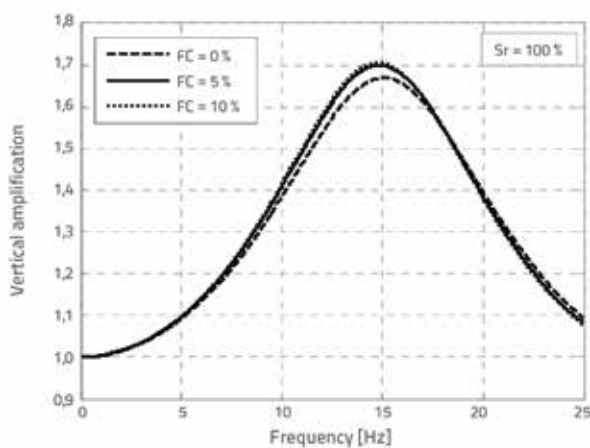

Figure 19. Effect of FC on vertical amplification (C_u = 5, n = 0.3, S_r = 100 %)

Furthermore, it should be mentioned that the variation of the fine content, FC, from 0 % to 10 % produces a decrease by 33.6 % and less than 2 % in P_1 wave velocity in partly and fully saturated cases, respectively (Figure 20a and 20b).
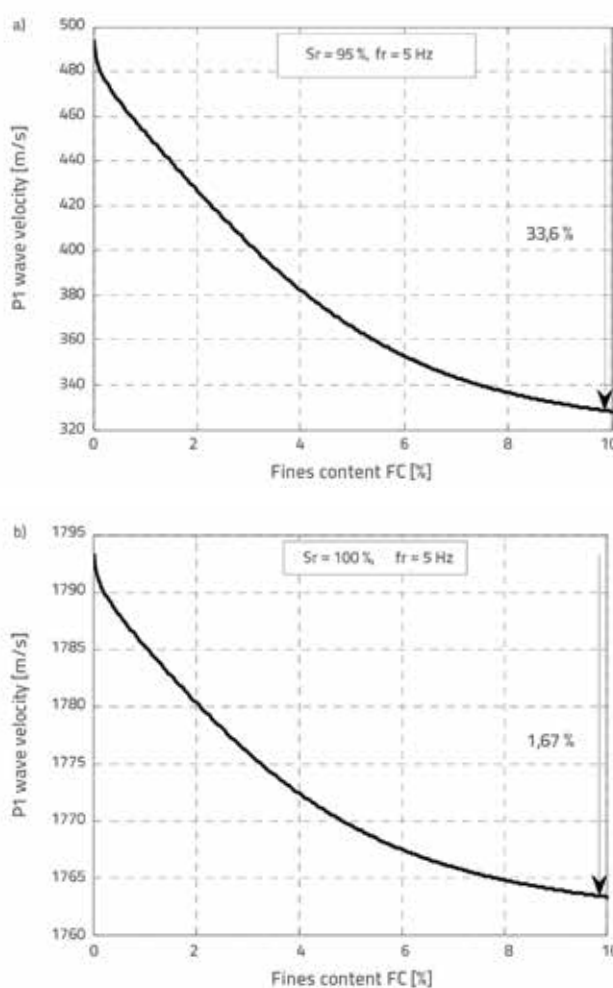

Figure 20. Effect of FC-values on P_1 wave velocity in: a) partly saturated porous soil; b) fully saturated porous soil (σ'_0 = 100 kPa, C_u = 5, n = 0.3)

Which confirms the little effect of stiffness variation on the vertical amplification in fully saturated soil. Moreover, the SV wave velocity also exhibits the same variation in the two cases of saturation (Figure 21).
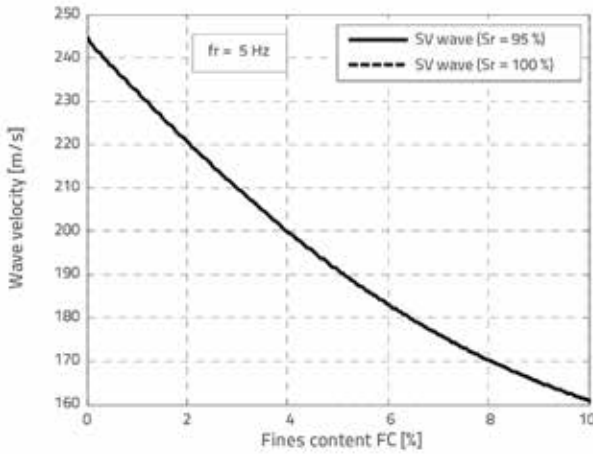
Figure 21. Effect of FC-values on SV wave velocity (σ'_0 = 100 kPa, C_u = 5, n = 0.3)
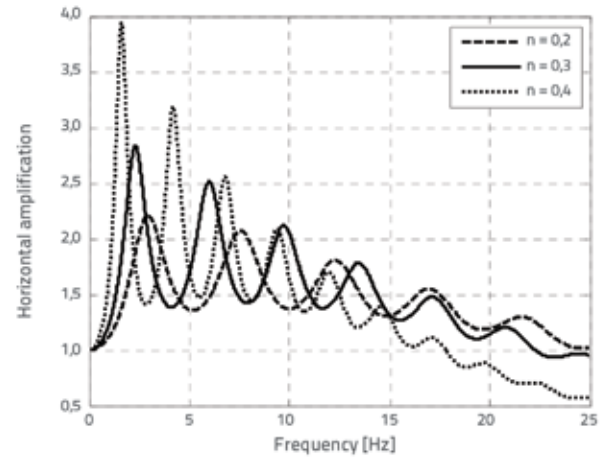

Figure 22. Effect of porosity n on horizontal amplification (C_u = 5, FC = 0 %)

4.1.5. Effect of porosity

Porosity is an important property that characterizes the porous media and often affects the flow conditions, as well as the physical properties of the solid skeleton such as shear

modulus. In this study, we consider that the shear modulus depends of porosity as described in the Wichtmann's model for sandy soil.

Figure 22 shows horizontal amplification for different porosity values n = 0.2, 0.3 and 0.4. It is clear that as the porosity
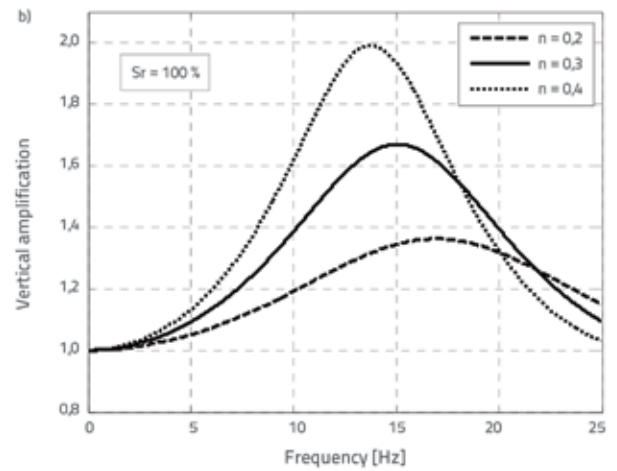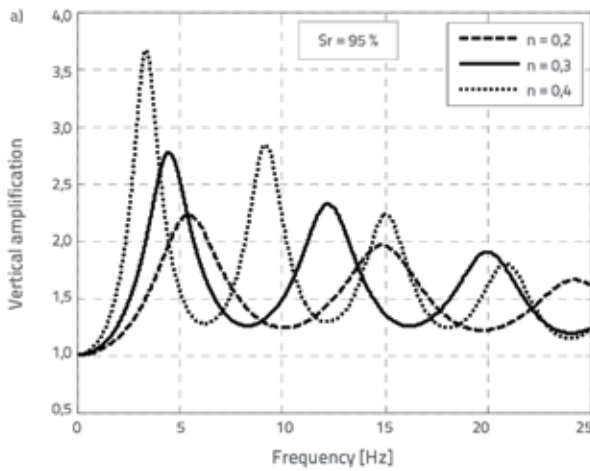

Figure 23. Effect of porosity n on vertical amplification in the cases of: a) partial saturation; b) full saturation (C_u = 5, FC = 0 %)
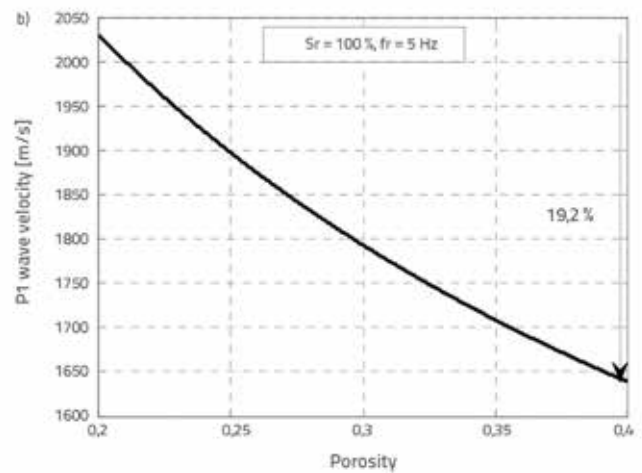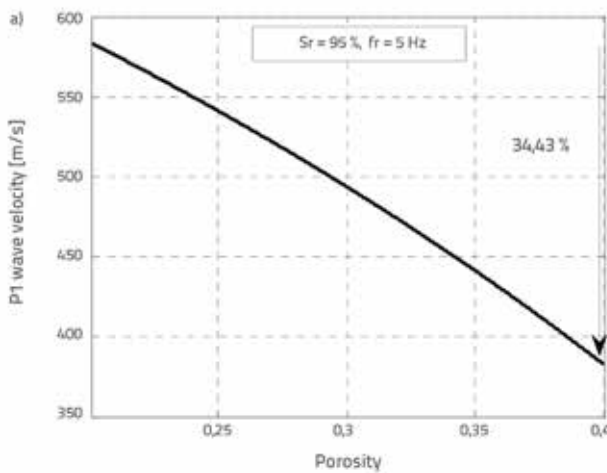

Figure 24. Effect of n-values on the P$_1$ wave velocity in: a) partly; b) fully saturated porous soil (σ'_0 = 100 kPa, C_u = 5, FC = 0 %)

increases the amplitude of peaks increases with a shift to low frequencies; the same comments are found for vertical amplification. This vertical amplification is more pronounced for the partly saturated soil compared to the fully saturated soil (Figure 23).

The phenomen explained above can be presented by variation of waves velocities. It is indicated in Figure 24 that the increase in porosity produces a significant influence on P_1 wave velocities, which decrease by 34.43 % and 19.2 % for the partly and completely saturated case, respectively. The SV wave velocity is also influenced, and the same trend is observed in the two cases of saturation (Figure 25).
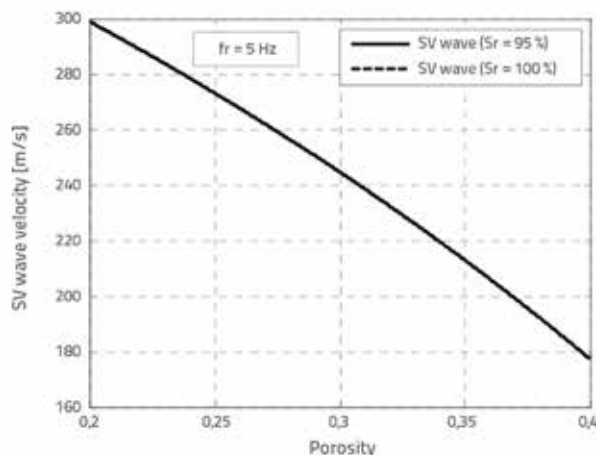

Figure 25. Effect of n-values on SV wave velocity (σ'_0 =100 kPa, C_u = 5, FC = 0 %)

It can be seen from the results of C_u and FC analysis that the P_1 wave velocity, and the vertical component of amplification in the fully saturated soil profile, are not influenced by the change in shear modulus; therefore, we can conclude that in this case the porosity effect cannot be due to the porosity-dependent stiffness of solid skeleton, but that it is due to porosity-dependent flow conditions.
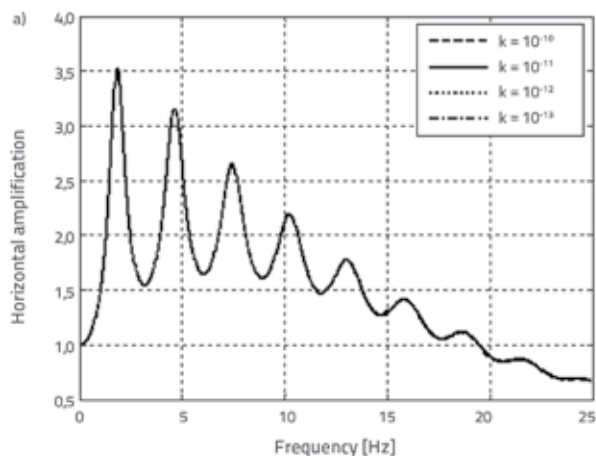
4.1.6. Effect of permeability

It is obvious that permeability is an important property in energy dissipation of saturated porous medium where the coefficient of dissipation (b = η/k)) depends on the intrinsic permeability of the skeleton and on fluid viscosity; this dissipation is due to the dynamic interaction between the solid and fluid phases [22]. In order to present the effect of permeability k (m^2), both vertical and horizontal amplification in fully water saturated soil are illustrated for k = 10^{-10}, 10^{-11}, 10^{-12} and 10^{-13} m^2 in Figure 26. As can be noticed, the bi-amplification is not influenced by the variation of permeability in this low range of k-values, because of the small relative pore fluid flow at this low permeability.

4.2. Equivalent-linear (EQL) site response analysis

The previous section focused on the linear analysis of a poroviscoelastic soil profile amplification, which assumed that the profile stiffness and damping are constants. However, the soil can exhibit a nonlinear behaviour [5, 39, 40], where dynamic properties of soil (shear modulus, G, and damping ratio, D) vary with shear strain.

In this study, the nonlinear site response is accounted for through an equivalent linear approach which uses an iterative analysis to estimate strain-compatible soil properties for each soil layer. This approach is only an approximation of the nonlinear hysteretic stress-strain behaviour of cyclically loaded soils.

In the equivalent linear approach, the response of soil profile is first calculated using the small strain stiffness and damping as outlined above for linear analysis. From this initial estimate, shear strain (γ) histories for each layer are computed, and then the value corresponding to 65 % of the peak shear strain of an earthquake motion is considered as the effective shear strain. Next, an iterative procedure is used to determine the degraded soil properties using the shear modulus reduction G/G_{max} and damping (D) curves for sand, prescribed in Figures 27-29, which are defined by the flowing modified Hardin and Drnevich equations [39] in Wichtmann et al. [7, 8] analysis:
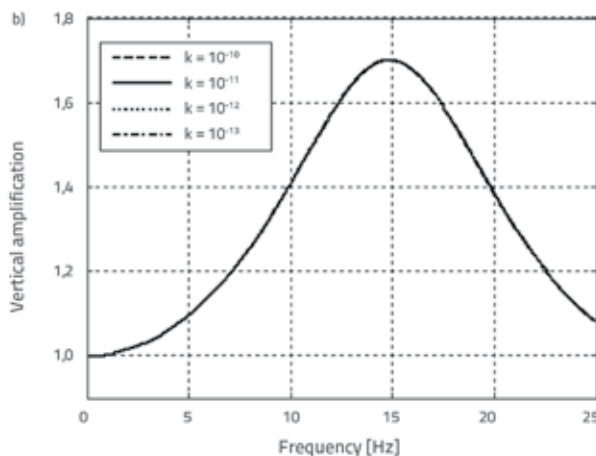

Figure 26. Effect of permeability k on: a) horizontal; b) vertical amplification (C_u = 5, FC = 5 %, n = 0.3)

$$\frac{G}{G_{max}} = \frac{1}{1 + \frac{\gamma}{\gamma_r}\left[1 + a_2\ \exp\left(-\frac{\gamma}{\gamma_r}\right)\right]} \tag{30}$$

$$D = 0.006 + 0.314 \frac{\frac{\gamma}{\gamma_r}\left[1 - 0.64\exp\left(-\frac{\gamma}{\gamma_r}\right)\right]}{1 + \frac{\gamma}{\gamma_r}\left[1 - 0.64\exp\left(-\frac{\gamma}{\gamma_r}\right)\right]} \tag{31}$$

The curve-fitting parameter a and the reference shear strain γ_r are defined as

$$a_2 = 1.070 \ln(C_u)\ \exp(0.053\ FC) \tag{32}$$

$$\gamma_r = \frac{\tau_{max}}{G_{max}} \tag{33}$$

For cohesionless soils, the maximum shear stress, τ_{max}, can be calculated from :

$$\tau_{max} = \sigma'_v \sqrt{\left(\frac{1 + K_0}{2}\sin\phi'\right)^2 - \left(\frac{1 - K_0}{2}\right)^2} \tag{34}$$

with the lateral stress coefficient, $K_0 = 1 - \sin\phi'$.

It can be noted that the shear modulus reduction G/G_{max} and damping (D) curves depend on confining pressure σ'_0 (Figure 27), the grain size distribution, C_u (Figure 28), and the non-cohesive fines content, FC (Figure 29).
During an earthquake, the motion is subjected to simultaneous seismic loads in both horizontal and vertical directions. This means that the soil profile is induced by incident P and SV waves at the same time, which implies that the P_1 waves propagate through a soil profile having the same degraded shear modulus due to shear strain produced by the SV wave propagation. On the basis of this assumption, and considering the fact that the damping ratio of P_1 wave is not yet clearly discussed, the same site conditions for the two cases of wave propagation (damping and shear modulus) are assumed in this paper.
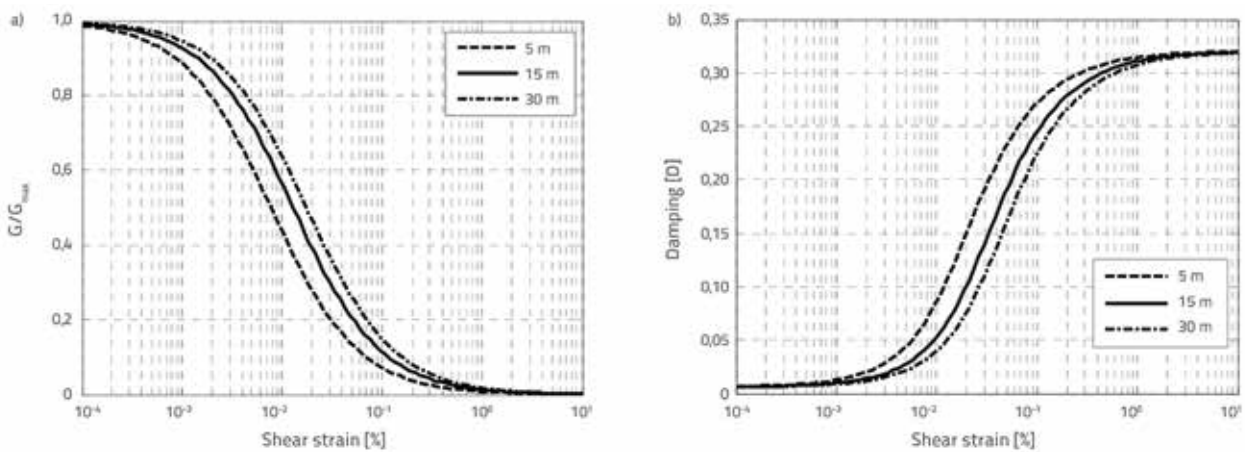

Figure 27. Effect of confining pressure σ'_0 on: a) shear modulus reduction curves; b) damping curves
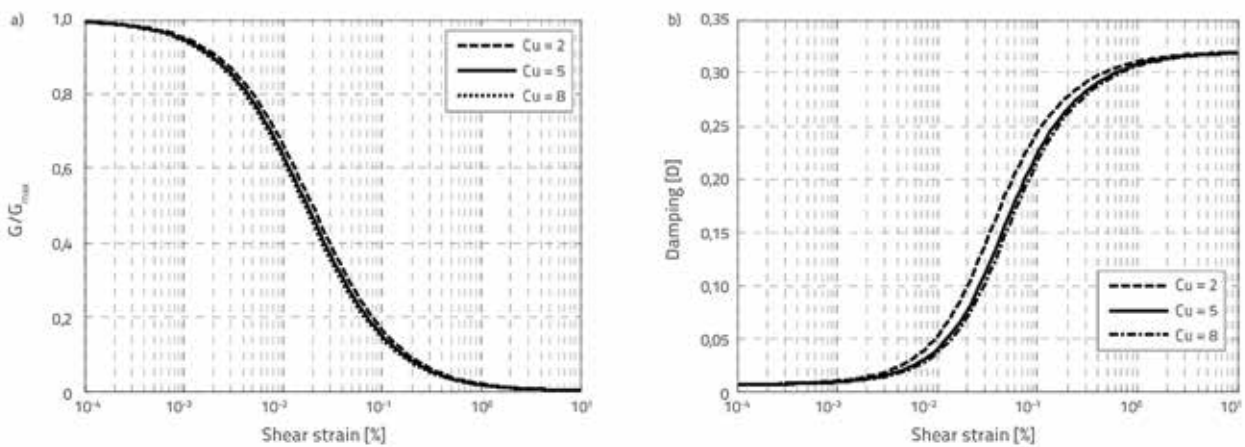

Figure 28. Effect of C_u-values on: a) shear modulus reduction curves; b) damping curves
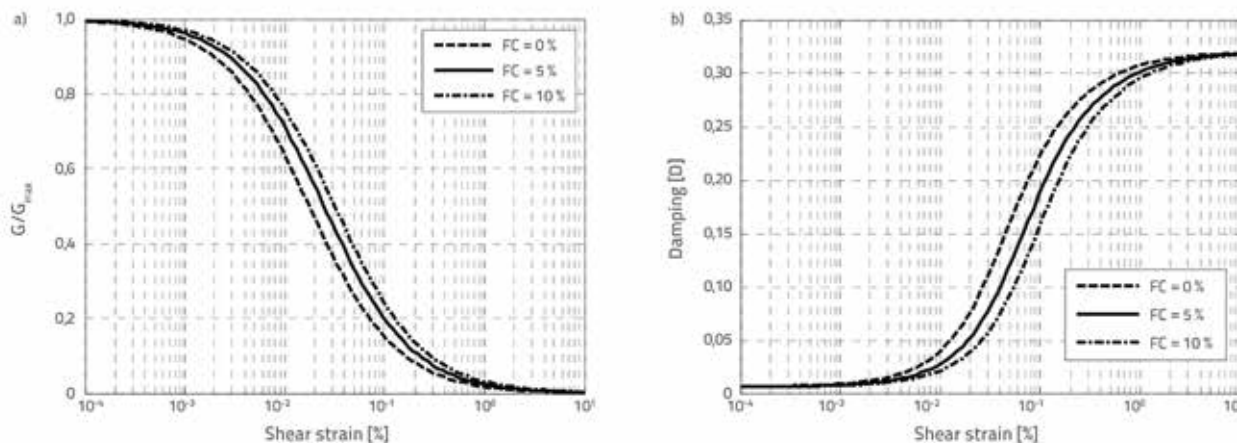
Figure 29. Effect of FC-values on: a) shear modulus reduction curves; b) damping curves

4.2.1. Input earthquake motion

To account for the effect of soil properties on nonlinear amplification of the saturated porous soil profile in horizontal and vertical directions, two components seismic accelerograms (North-South and up–down directions) are selected in this study as a rock outcropping motion to excite the soil profile. These motions were recorded during the El Centro (1940) earthquake, where the values of *PGA* are 0.28g and 0.178g for the horizontal and vertical motions, respectively (Figure 30).

4.2.2. Analysis of amplification functions

In order to approximately estimate the nonlinear response of the soil profile, an equivalent-linear site response analysis is used in this section. It can be seen from figures 31 and 32 that the increase of C_u, *FC* and *n*-values amplifies the peaks amplitudes with a shift to low frequencies for the horizontal amplification, as well as for the vertical one in the partly saturated soil profile case. For instance, the increase of C_u-values from $C_u = 2$ to $C_u = 8$ (Figure 31a and 32a) increases the amplitude of the first peak by 34.3 %
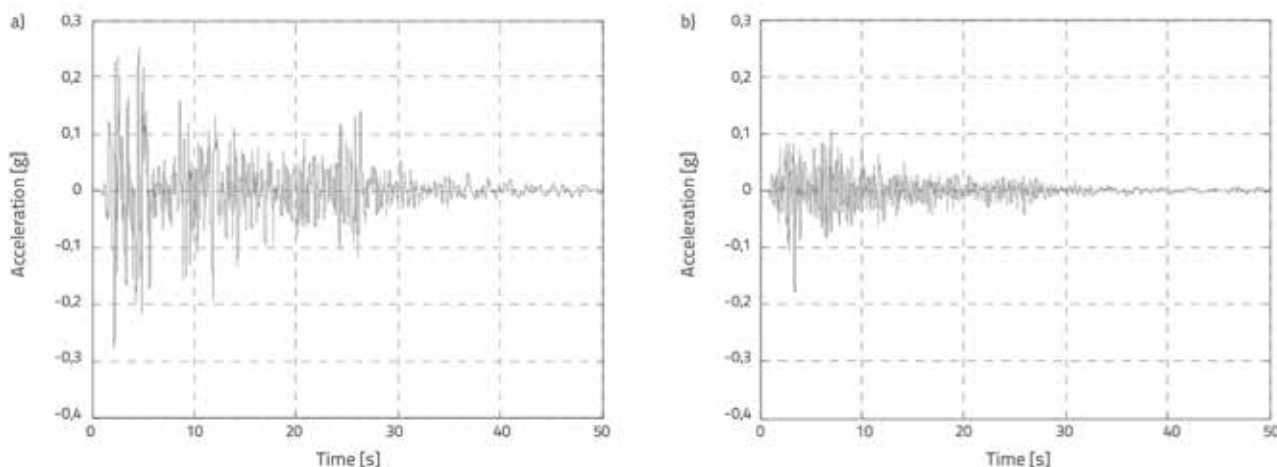

Figure 30. Time histories for El Centro acceleration 1940: a) Horizontal component; b) Vertical component
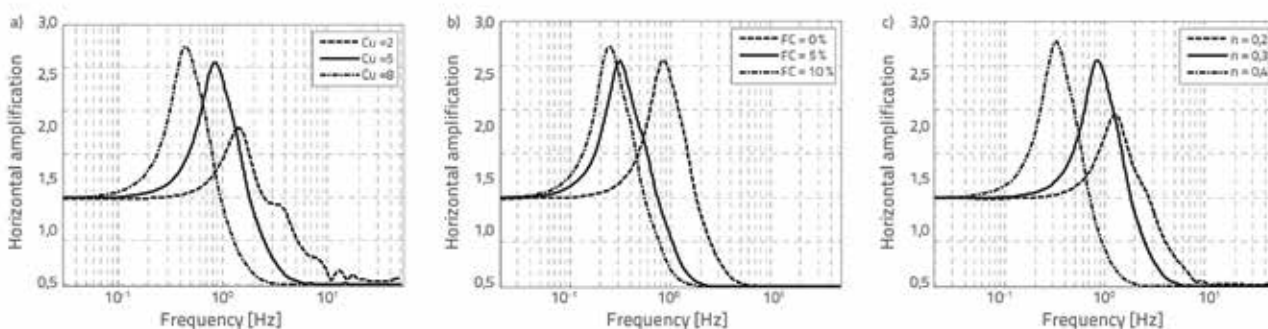

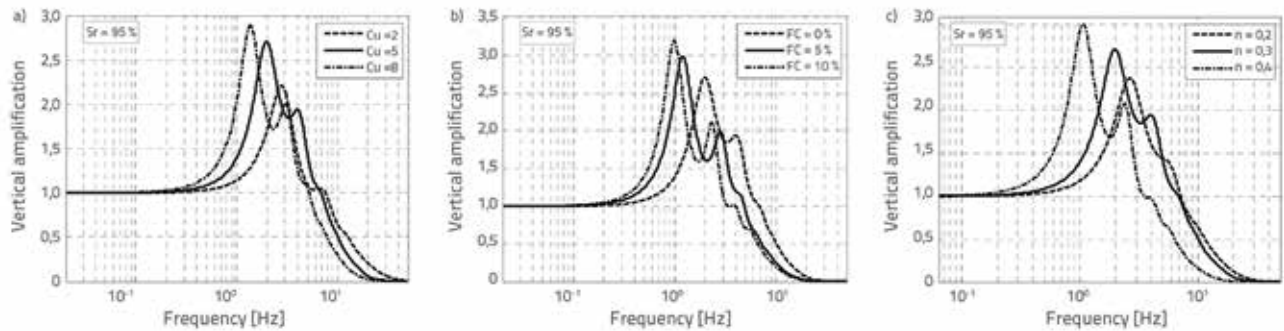Figure 31. Effect of: a) C_u-values: b) FC-values: c) n-values on nonlinear horizontal amplification

Figure 32. Effect of: a) C_u-values: b) FC-values: c) n-values on nonlinear vertical amplification (partly saturated soil)
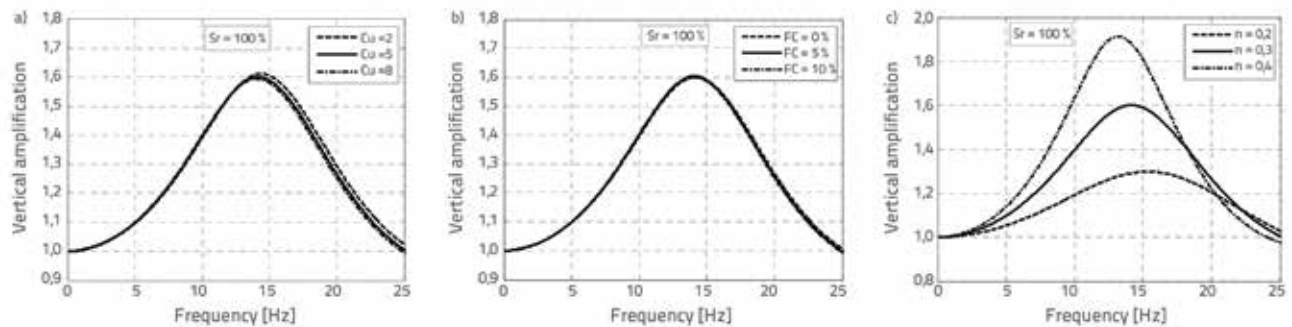

Figure 33. Effect of: a) C_u-values: b) FC-values: c) n-values on nonlinear vertical amplification (fully saturated soil)

and 23.87 % with a shift to low frequencies by 0.97 Hz and 1.43 Hz for both horizontal and vertical amplifications, respectively. Moreover, in the case of fully saturated soil profile the vertical response is not influenced by all C_u and FC values (Figure 33a and 33b). Thus, the increase of porosity induced an increase of amplitude with a shift to low frequencies (Figure 33c). In addition, it is interesting to mention that the vertical response exhibits an identical behaviour to that exhibited in linear analysis, which implies that vertical amplification is not influenced by nonlinear behaviour in the fully saturated soil profile.

5. Conclusions

The effect of soil properties on linear and nonlinear amplification function of an inhomogeneous poroviscoelastic soil profile in both horizontal and vertical directions is investigated in this paper, by applying the Biot's two-phase media theory and using an analytical approach based on the exact stiffness matrix method, and by assuming that the incoming seismic wave consists of inclined P-SV waves. It is taken into consideration that mechanical properties increase with depth, according to the Wichtmann's model which considers the effect of grain size distribution, porosity and fines content on the small strain shear modulus, the shear modulus reduction, and damping curves. The main conclusions of this study are as follows:
- When the SV wave presents an angle of incidence different from zero in saturated porous media, the horizontal amplification function exhibits an amplitude less than calculated in the single-phase medium, which can be explained by generation of the P_2-wave. The effect of incidence angle on vertical response is negligible.

- Furthermore, saturation did not influence the horizontal amplification, but it strongly affected the vertical amplification, where a slight decrease below complete saturation induced a significant amplification and shift to low frequencies. This behaviour is due to the strong variation of the pore fluid modulus, K_f with saturation.
- The bi-amplification is not influenced by variation of permeability in the low range of k-values.
- The coefficient of uniformity, C_u, and fines content, FC, exert an important influence on vertical amplification in partly saturated soil profile in case of both linear and nonlinear soil behaviour, but their effect is negligible when $S_r = 100$ %.
- The porosity also has a strong effect on vertical response in the case of partial saturation; yet, its impact is less significant in the case of complete saturation.
- These results indicate that variation of the vertical response and P-wave velocity in the case of partly saturated soil is related to mechanical properties; this variation is due to the flow conditions in case of complete saturation. The nonlinear vertical response exhibits an identical behaviour to that in linear analysis when $S_r = 100$ %, which implies that vertical response is not influenced by nonlinear behaviour of the fully saturated soil profile.
- The coefficient of uniformity, fines content and porosity also have a significant effect on horizontal amplification in both linear and nonlinear soil behaviour.

The results of this study indicate that there is a significant effect of local site properties on the poroviscoelastic soil amplification in both vertical and horizontal direction. Some improvements can be introduced to this research through further study of the response spectral ratio (V/H) and the use of the soil properties as spatial random fields.

REFERENCES

[1] Trifunac, M.D.: Site conditions and earthquake ground motion–A review, Soil Dynamics and Earthquake Engineering, 90 (2016), pp. 88-100, https://doi.org/10.1016/j.soildyn.2016.08.003

[2] Hardin, B.O., Black, W.L.: Vibration Modulus of Normally Consolidated Clays, Journal of the Soil Mechanics and Foundations Division, 94 (1968) 2, pp. 353-369.

[3] Seed, H.B., Idriss, I.M.: Soil Modulus and Damping Factors for Dynamic Response Analysis, Technical Report EERC70–10, Earthquake Engineering Research Center, University of California, Berkeley, 1970.

[4] Stokoe, K.H., Woods, R.D: In situ shear wave velocity by cross-hole method, Journal of the Soil Mechanics and Foundations Division, 98 (1972) 5, pp. 443-460.

[5] Menq, F.Y.: Dynamic Properties of Sandy and Gravelly Soils, PhD thesis, Texas University, USA. 2003.

[6] Wichtmann, T., Triantafyllidis, T.: On the influence of the grain size distribution curve of quartz sand on the small strain shear modulus G_{max}, Journal of Geotechnical and Geoenvironmental Engineering, 135 (2009) 10, pp. 1404–1418.

[7] Wichtmann, T., Triantafyllidis, T.: Small-strain constrained elastic modulus of clean quartz sand with various grain size distribution, Soil Dynamics and Earthquake Engineering, 55 (2013), pp. 130-139.

[8] Wichtmann, T., Hernandez, M., Triantafyllidis, T.: On the influence of a non-cohesive fines content on small strain stiffness, modulus degradation and damping of quartz sand, Soil Dynamics and Earthquake Engineering, 69 (2015), pp. 103–114, https://doi.org/10.1016/j.soildyn.2014.10.017

[9] Idriss, I.M., Seed, H.B.: Seismic response of horizontal layers, Journal of the Soil Mechanics and Foundations Division, ASCE, 94(SM4): 1003-31 (1968).

[10] Dobry, R., Whitman, R., Roesset, J.M.: Soil properties and the one-dimensional theory of earthquake amplification, Research Report R71-18, Department of Civil Engineering, Massachusetts Institute of Technology, 1971.

[11] Gazetas, G.: Vibrational Characteristics of Soil Deposits with Variable Wave Propagation Velocity, International Journal for Numerical and Analytical Methods in Geomechanics, 6 (1982), pp. 1–20.

[12] Hadid, M., Afra, H.: Sensitivity Analysis of Site Effects on Response Spectra of Pipelines, Soil Dynamics and Earthquake Engineering, 20 (2000), pp. 249–260.

[13] Afra, H., Pecker, A.: Calculation of free field response spectrum of a non-homogeneous soil deposit from bed rock response spectrum, Soil Dynamics and Earthquake Engineering, 22 (2002) 2, pp. 157-165.

[14] Travasarou, T., Gazetas, G.: On the Linear Response of Soils with Modulus Varying as a Power of Depth-the Maliakos Marine Clay, Soils and Foundations, 44 (2004) 5, pp. 85-93.

[15] Rovithis, E.N., Parashakis, H., Mylonakis, G.E.: 1D harmonic response of layered inhomogeneous soil: analytical investigation, Soil Dynamics and Earthquake Engineering, 31 (2011), pp. 879–90, https://doi.org/10.1016/j.soildyn.2011.01.007

[16] Mylonakis, G.E., Rovithis, E., Parashakis, H.: 1D harmonic response of layered inhomogeneous soil: exact and approximate analytical solutions, In Computational Methods in Earthquake Engineering, pp. 1-32, Springer Netherlands, 2013.

[17] Vrettos, C.: Dynamic response of soil deposits to vertical SH waves for different rigidity depth-gradients, Soil Dynamics and Earthquake Engineering, 47 (2013), pp. 41–50, https://doi.org/10.1016/j.soildyn.2012.04.003

[18] Durante, M.G., Karamitros, D., Di Sarno, L., Sica, S., Taylor, C.A., Mylonakis, G., Simonelli, A.L.: Characterisation of shear wave velocity profiles of non-uniform bi-layer soil deposits: analytical evaluation and experimental validation, Soil Dynamics and Earthquake Engineering, 75 (2015), pp. 44–54, Https://doi.org/10.1016/j.soildyn.2015.03.010

[19] Jamshidi, C.R., Aminzadeh, B.T.S.: Site response of heterogeneous natural deposits to harmonic excitation applied to more than 100 case histories, Earthquake Engineering And Engineering Vibration, 15 (2016) 2, pp. 341-356, https://doi.org/10.1007/s11803-016-0326-0

[20] Biot, M.A.: Theory of Propagation of Elastic Waves in a Fluid-Saturated Porous Solid-Low Frequency Range, Journal of Acoustic Society of America, 28 (1956) 2, pp. 168-178.

[21] Biot, M.A.: Theory of Propagation of Elastic Waves in a Fluid-Saturated Porous Solid-Higher Frequency Range, Journal of Acoustic Society of America, 28 (1956) 2, pp. 179-191.

[22] Biot, M.A.: Mechanics of Deformation and Acoustic Propagation in Porous Media, Journal of Applied Physics, 33 (1962) 4, pp. 1482-1498.

[23] Ke, L.L., Wang, Y.S., Zhang, Z.M.: Propagation of Love waves in an inhomogeneous fluid-saturated porous layered half-space with properties varying exponentially, Journal of Engineering Mechanics, 131 (2005) 12, pp. 1322–1328, https://doi.org/10.1061/ASCE0733-9399(2005)131:12(1322)

[24] Ke, L.L., Wang, Y.S., Zhang, Z.M.: Love wave in an inhomogeneous fluid-saturated porous layered half space with linearly varying properties, Soil Dynamics and Earthquake Engineering, 26 (2006), pp. 574–581, https://doi.org/10.1016/j.soildyn.2006.01.010

[25] Zhou, F.X., Lai, Y.M., Song, R.X.: Propagation of plane wave in non-homogeneously saturated soils, Science China Technological Sciences, 56 (2013) 2, pp. 430-440, https://doi.org/10.1007/s11431-012-5106-0

[26] Zhou, F.X., Ma, Q.: Propagation of Rayleigh waves in fluid-saturated non-homogeneous soils with the graded solid skeleton distribution, International Journal For Numerical And Analytical Methods In Geomechanics, 2016, https://doi.org/10.1002/nag.2491.

[27] Zhou, F.X.: Transient Dynamic analysis of gradient-saturated viscoelastic porous media, Journal of Engineering Mechanics, 140 (2013) 4, pp. 1–9, https://doi.org/10.1061/(ASCE)EM.1943-7889.0000706

[28] Rajapakse, R.K.N.D., Senjuntichai, T.: Dynamic response of a multi-layered poroelastic medium, Earthquake Engineering and Structural Dynamic, 24 (1995), pp. 703-722.

[29] Yang, J., Sato, T.: Influence of Viscous Coupling on Seismic Reflection and Transmission in Saturated Porous Media, Bulletin of the Seismological Society of America, 88 (1998) 5, pp. 1289-1299.

[30] Lin, CH., Lee, V.W., Trifunac, M.D.: The reflection of plane waves in a poroelastic half-space saturated with inviscid fluid, Soil Dynamics and Earthquake Engineering, 25 (2005), pp. 205–223, https://doi.org/10.1016/j.soildyn.2004.10.009

[31] Liang, J., Fu, J., Todorovska, M.I., Trifunac, M.D.: In-plane soil–structure interaction in layered,fluid-saturated, poroelastic half-space I: Structural response, Soil Dynamics and Earthquake Engineering, 81 (2016), pp. 84-111, https://doi.org/10.1016/j.soildyn.2015.10.018

[32] Wichtmann, T., Triantafyllidis, T.: On the influence of the grain size distribution curve on P-wave velocity,constrained elastic modulus Mmax and Poisson's ratio of quartz sands, Soil Dynamics and Earthquake Engineering, 30 (2010), pp. 757–766, https://doi.org/10.1016/j.soildyn.2010.03.006

[33] Argeso, H., Mengi, Y.: A frequency domain boundary element formulation for dynamic interaction problems in poroviscoelastic media, Computational Mechanics, 53 (2014) 2, pp. 215–237 (2014), https://doi.org/10.1007/s00466-013-0903-2

[34] Yoshinori Iwasaki, and Masaru Tai.: Strong motion records at Kobe Port Island, Soils and foundations, pp. 29-40, 1996.

[35] Jorge Aguirre.: Non-linear site effects at port island vertical array during 1995 Hyogo-Ken Nanbu earthquake, Eleventh world conference on earthquake engineering,1996

[36] Han, B., Zdravkovic, L., Kontoe, S.: Numerical and analytical investigation of compressional wave propagation in saturated soils, Computers and Geotechnics, 75 (2016), pp. 93–102, https://doi.org/10.1016/j.compgeo.2016.01.019

[37] Polito, C.P.: The Effect of Non-plastic and Plastic Fines on the Liquefaction of Sandy Soils, PhD Thesis, Virginia Polytechnic Institute and State University, 1999.

[38] Belkhatir, M., Schanz, T., Arab, A., Della, N.: Experimental Study on the Pore Water Pressure Generation Characteristics of Saturated Silty Sands, Arabian Journal for Science and Engineering 39 (2014) 8, pp. 6055-6067, https://doi.org/10.1007/s13369-014-1238-9

[39] Hardin, B.O., Drnevich, V.P.: Shear modulus and damping in soils: design equations and curves, Journal of the Soil Mechanics and Foundations Division, 98 (1972) SM7, pp. 667–92.

[40] Darendeli, M.B.: Development Of A New Family Of Normalized Modulus Reduction And Material Damping Curves, Ph.D thesis, Texas University, USA, 2001.